



CHEMISTRY & BIODIVERSITY

Accepted Article

Title: Design, synthesis and biological evaluation of xanthone derivatives for possible treatment of Alzheimer's disease based on multi-target strategy

Authors: Aihong Yang, Qiao Yu, Hui Ju, Lulu Song, Xiaodi Kou, and Rui Shen

This manuscript has been accepted after peer review and appears as an Accepted Article online prior to editing, proofing, and formal publication of the final Version of Record (VoR). This work is currently citable by using the Digital Object Identifier (DOI) given below. The VoR will be published online in Early View as soon as possible and may be different to this Accepted Article as a result of editing. Readers should obtain the VoR from the journal website shown below when it is published to ensure accuracy of information. The authors are responsible for the content of this Accepted Article.

To be cited as: *Chem. Biodiversity* 10.1002/cbdv.202000442

Link to VoR: <https://doi.org/10.1002/cbdv.202000442>

Design, synthesis and biological evaluation of xanthone derivatives for possible treatment of Alzheimer's disease based on multi-target strategy

Aihong Yang, Qiao Yu, Hui Ju, Lulu Song, Xiaodi Kou* and Rui Shen*

School of Chinese Materia Medica, Tianjin University of Traditional Chinese Medicine, Tianjin 301617.

**E-mail address for correspondence: xiaodikou2013@163.com, shenr2016@126.com.*

Four xanthone derivatives were synthesized and evaluated as acetylcholinesterase inhibitors (AChEIs) with metal chelating ability and antioxidant ability against Alzheimer's disease (AD). Most of them exhibited potential acetylcholinesterase (AChE), butylcholinesterase (BuChE) inhibitory, antioxidant and metal chelating properties. Among them, 3-(2-(pyrrolidinyl)ethoxy)-1-hydroxy-9H-xanthen-9-one (**2**) had the highest ability to inhibit AChE and displayed high selectivity towards AChE ($IC_{50}=2.403\pm0.002\ \mu\text{M}$ for AChE and $IC_{50}=31.221\pm0.002\ \mu\text{M}$ for BuChE). And it was also a good antioxidant ($IC_{50}=2.662\pm0.003\ \mu\text{M}$). Enzyme kinetic studies showed that compound **2** was a mixed-type inhibitor, which could interact simultaneously with the catalytic anionic site (CAS) and the peripheral anionic site (PAS) of AChE. Interestingly, the copper complex (**2**- Cu^{2+}) showed more significant inhibitory activity for AChE ($IC_{50}=0.934\pm0.002\ \mu\text{M}$) and antioxidant activity ($IC_{50}=1.064\pm0.003\ \mu\text{M}$). Molecular dockings were carried out for the four xanthone derivatives in order to further investigate the binding modes. Finally, the blood-brain barrier (BBB) penetration prediction indicated that all compounds might penetrate BBB. These results suggested that compound **2** was promising AChEI with metal chelating ability and antioxidant ability for the further investigation.

Keywords: Xanthone • Anti-ChE activity • Anti-oxidant activity • Metal chelation

Introduction

Alzheimer's disease (AD) is a progressive neurological disease leading to memory impairment.^[1] AD is the main cause of dementia. The amount of patients is increasing year by year. It is estimated that there will be one in every 85 people to suffer AD by 2050.^[2] AD also induced a great amount of economic loss, the overall cost for AD was estimated to be 818 billion dollars in 2015, with an increase of 35.3% compared to 2010 and the datum is expected to double by 2030.^[3] Although considerable researches have been devoted to understanding and modulating the pathogenetic mechanisms of AD, the etiology of AD still remains unclear. Diverse factors have been demonstrated to play crucial roles in the pathogenesis of AD, including deficits of choline,^[4] oxidative stress,^[5] dyshomeostasis of biometals^[6] and formation of β -amyloid ($\text{A}\beta$) deposits,^[7] etc. Due to the complex pathogenesis of AD, multi-target-directed ligands (MTDLs) strategy has been applied in the search for potential anti-AD drugs.^[8,9]

In fact, the different pathogenetic factors of AD are interconnected. The peripheral anionic site (PAS) of acetylcholinesterase (AChE) can accelerate the formation of $\text{A}\beta$ aggregation and amyloid fibril. The

Chem. Biodiversity

interaction between A β and the PAS produces stable AChE-A β complexes, which are more toxic than A β peptide aggregates.^[10] Metal ions, such as Cu²⁺ and Fe³⁺ can stimulate the generation of reactive oxygen species (ROS) and lead to oxidative stress.^[11,12] Oxidative stress with degradation of several cellular biomolecules including nucleic acids, proteins, and lipids is an event that precedes the appearance of other pathological hallmarks of AD, such as senile plaques and neurofibrillary tangles.^[13,14] The cholinergic hypothesis proposed by scientists has been proved to be a clinically viable strategy. In recent years, the new acetylcholinesterase inhibitors (AChEIs) have attracted many researchers.^[15,16]

Xanthenes, widely exist in *Polygalaceae*, *Guttiferae*, *Gentianaceae* and some families of fungi and lichens, are well-known natural compounds.^[17,18] They display a wide range of biological activities, such as anti-inflammatory,^[19] antitumour,^[20] antioxidant^[21] and inhibition of cholinesterase,^[22] which has led to the xanthenes being designated as 'privileged structures'.^[23] Especially, xanthone derivatives as cholinesterase inhibitors have received significant attention in the recent years.^[24,25]

In this work, four xanthone derivatives with tertiary amine side chains have been synthesized as novel effective candidates against AD. The rational design of these xanthone derivatives is shown in Figure 1. Firstly, most of the reported or clinically used reversible AChEIs are tertiary amines (such as donepezil and rivastigmine) or quaternary ammonium salt (such as neostigmine). So tertiary and quaternary amines are valuable candidates for the development of AChEI medicines. In this work, we designed the double sites inhibitor and chose xanthone to interact with PAS and the tertiary amine to interact with CAS. Secondly, the active sites of AChE include PAS, CAS and a hydrophobic area. In consideration of the distance of the active sites in AChE, the flexible and hydrophobic carbon chain consisting of two or three carbon atoms is suitable to work as the linker. In addition, the linker length with two carbon atoms is more likely to penetrate the blood-brain barrier than compounds with longer carbon chains. Therefore, in this work, xanthone derivatives with two carbon chain lengths were selected as the research objects. Thirdly, the 1-hydroxy group and carbonyl group on the xanthone scaffold can work as the chelating sites to metal ions. Finally, the phenol and amine moieties can be good antioxidants. So, these compounds may contain the properties of AChE inhibition, metal chelating, and antioxidant at the same time. Furthermore, the absorption and blood-brain barrier (BBB) permeability were predicted and molecular dockings were studied.

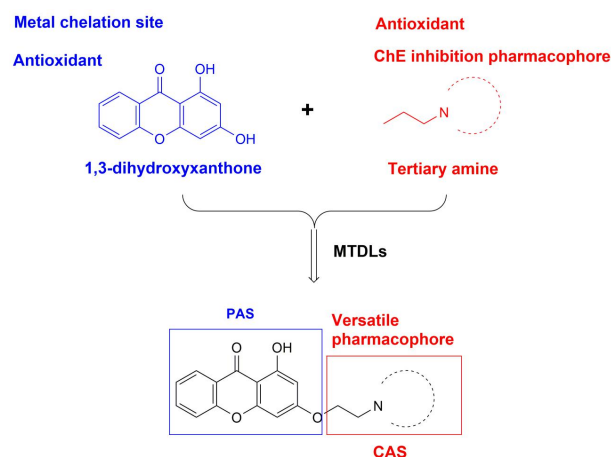


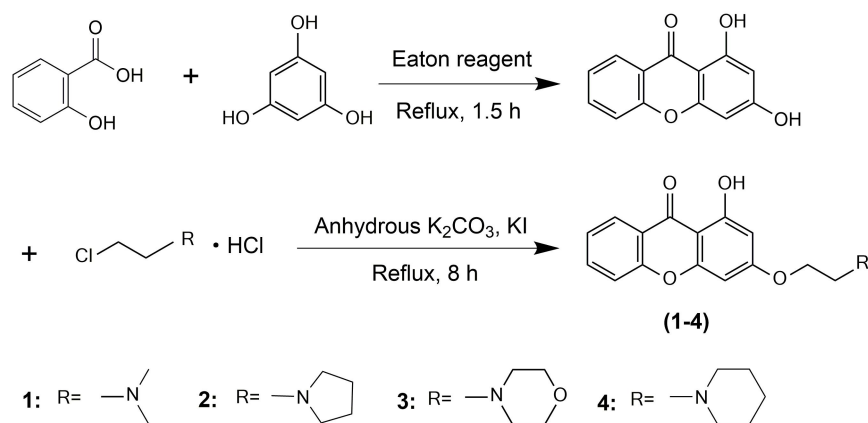
Figure 1. Rational design of xanthone derivatives.

Chem. Biodiversity

Results and Discussion

Synthesis

1,3-Dihydroxy xanthone (1,3-DHX) was prepared according to the literatures.^[26] Amination of 1,3-DHX with amine alkyl halides in acetone was carried out according to the literatures^[27] with some improvements (Scheme1). The structures of all compounds were confirmed by ¹H NMR, ¹³C NMR, MS, Elemental analyses and IR.^[28]



Scheme 1. Synthesis of compounds **1-4**.

Metal-chelating properties

In compounds **1-4**, 1-hydroxy and 9-carbonyl can work as binding sites to chelate with metal ions, which can be confirmed by the disappearance of 1-hydroxy peak at 12.71 ppm and the shift of peaks on the xanthone ring in the ¹H NMR of the zinc complex. The ¹H NMR spectra were shown in Figure S1 of Supporting Information. To further study the chelating ability of compounds, a series of absorption spectra of **1-4** titrated with Cu²⁺ or Fe³⁺ were collected. Compound **2** was taken as an example and the results were shown in Figure 2. The black line is full-wavelength UV scan curve of **2** without metal ions. The curves of other colors are full-wavelength scans of different mole ratios of metal and compound **2**. Compound **2** exhibits a maximum absorption at 236 nm and moderate-intensity absorption at 303 or 304 nm. When Cu²⁺ or Fe³⁺ was added into the solution, a new peak appeared at 269 nm, indicating the formation of the copper or iron complex. To confirm the component of the complex, the binding stoichiometry of compound **2** with Cu²⁺ or Fe³⁺ was determined by measuring the changes in absorption at 269 nm. As shown in the scatter plot in Figure 2, the results of titration analysis indicate that the stoichiometric ratio of complex is 2:1.

In addition, the experimental results of metal chelating ability of the other compounds were similar to **2** (the titration figures were shown in Figure S2-S4 of Supplemental Information).

Chem. Biodiversity

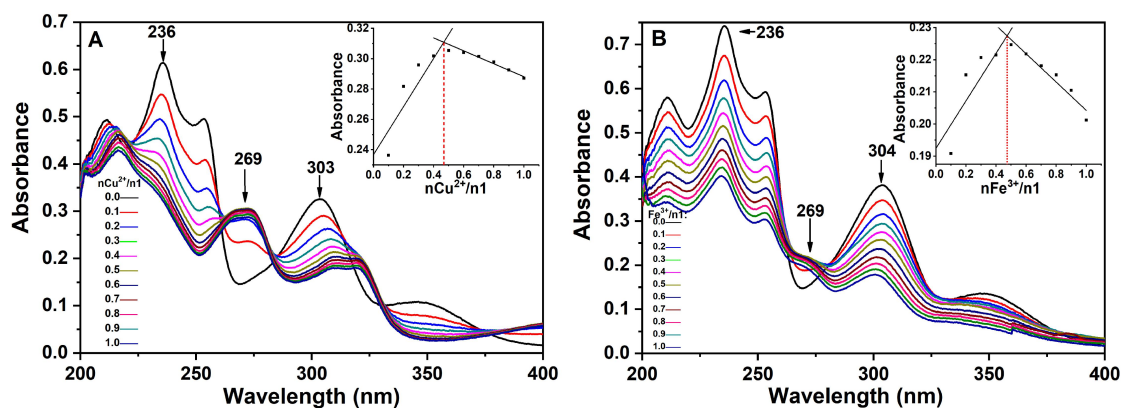


Figure 2. Metal chelating capacity of **2**: the absorption spectra of **2**-Cu²⁺ (A) and **2**-Fe³⁺ (B) in absolute ethyl alcohol and determination of the stoichiometry of **2**-Cu²⁺ or **2**-Fe³⁺ complex (embedding figure).

Cholinesterase inhibitory activity

The AChE (from *electric eel*) and BuChE (from equine serum) inhibition effects of **1-4** and **2**-Cu²⁺ were determined by Ellman method.^[29] Tacrine was applied as standard compound for comparison.^[9] Tacrine, a classical AChE inhibitor, could bond to the important amino acids Phe330, Prp84 and Ser122 of AChE through π -cation and π - π interactions (Figure S5 of Supporting Information). The IC₅₀ values and selectivity index were presented in Table 1. In vitro assays proved that all of the compounds had higher inhibitory activities against AChE than 1,3-DHX. **2** and **4** effectively inhibited AChEs in the micromolar range, which were comparable to tacrine. **1** exhibited moderate inhibitory activity for AChE. However, **3** showed weak inhibitory ability. Interestingly, the **2**-Cu²⁺ complex displayed stronger inhibitory activity for AChE than **2**. In addition, the results of BuChE inhibitory activity of **1-4** showed that **2** had high inhibition selectivity for AChE over BuChE. While **4** might act as a potent dual inhibitor of AChE and BuChE.

Table 1. AChE and BuChE inhibitory activity and antioxidant activity.

Compound	AChE IC ₅₀ (μ M) ^[a]	BuChE IC ₅₀ (μ M) ^[a]	Selective Index ^[b]	Scavenging·OH IC ₅₀ (μ M) ^[a]
1	19.731 \pm 0.003	37.250 \pm 0.021	1.888	3.841 \pm 0.004
2	2.403 \pm 0.002	31.221 \pm 0.002	12.992	2.662 \pm 0.003
3	156.310 \pm 0.004	>200	—	12.399 \pm 0.012
4	2.615 \pm 0.004	2.816 \pm 0.004	1.076	6.448 \pm 0.005
2 -Cu ²⁺	0.934 \pm 0.002	—	—	1.064 \pm 0.003
Tacrine	0.529 \pm 0.003	0.261 \pm 0.001	0.493	—
Vitamin C	—	—	—	7821 \pm 0.004
1,3-DHX	>200	>200	—	—

^[a]IC₅₀: 50% inhibitory concentration (means \pm SEM of three times).

^[b]Selectivity Index = IC₅₀ (BuChE)/IC₅₀ (AChE)

Kinetic study of AChE inhibition

Enzyme kinetic study was carried out to investigate the inhibitory mechanism of compound **2** based on the above results. Inhibition mechanism was analyzed with Lineweaver–Burk Plots. As shown in Figure 3, all straight lines are intersected in the second quadrant. According to the Michaelis–Menten equation,^[30] as the

Chem. Biodiversity

sample concentration increased, V_{\max} decreased, K_m increased, and K_m/V_{\max} increased. It was showed a mixed-type inhibition. The K_i (slope) and K_i' (intercept) value of compound **2** were calculated.^[31] The K_i and K_i' values were estimated as 3.3824 μM and 4.9139 μM . The value of α (K_i/K_i') < 1 further indicated **2** was a competitive/noncompetitive mixed-type inhibitor.^[32]

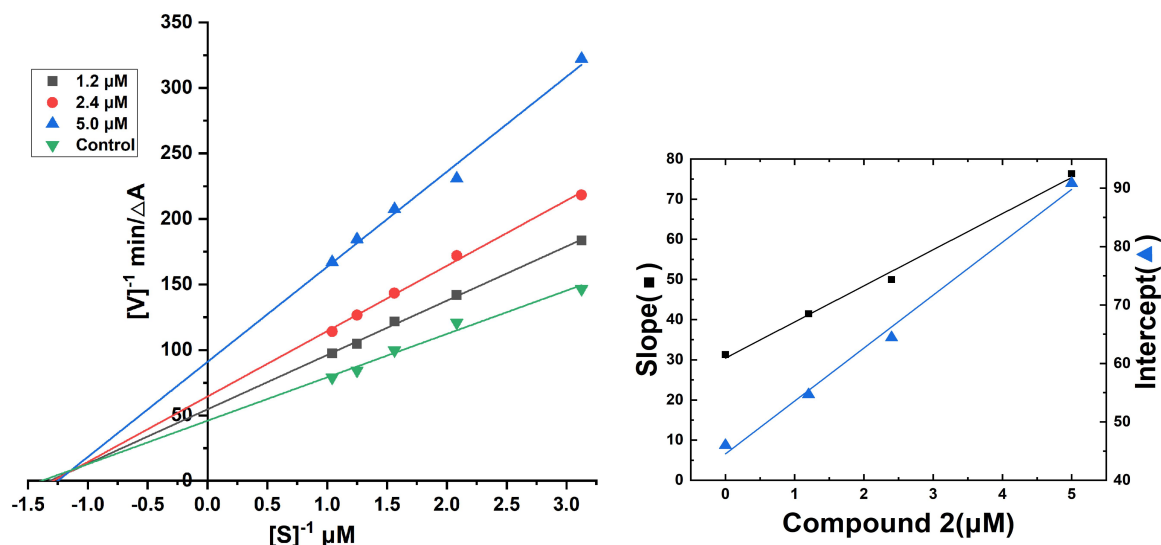


Figure 3. Kinetic study of the mechanism of AChE inhibition activity of compound **2**.

Antioxidant ability

Antioxidative activity is considered valuable therapeutic pathway against AD. Hydroxyl radical ($\cdot\text{OH}$) is the major ROS in human body. The $\cdot\text{OH}$ scavenging activities of compounds **1-4** and **2-Cu²⁺** were examined and shown in Table 1. With vitamin C as a control,^[33] the antioxidant capacity tests were conducted with the Fenton reaction.^[34] As shown in Figure 4, they show exceptional excellent antioxidant activities compared with vitamin C, of which the IC_{50} value is 7821 μM . The excellent antioxidative activity of compounds **1-4** might come from the phenol moiety.^[30] It might also come from the introduced amine moieties since amines are notoriously easy to be oxidized by donating the lone pair. Amines can even be oxidized during storage in contact with the air.^[35] So compounds **1-4** can act as good antioxidants when ROS present. While the increased antioxidant activity of **2-Cu²⁺** could be attributed to the synergetic effect of metal and the ligand.

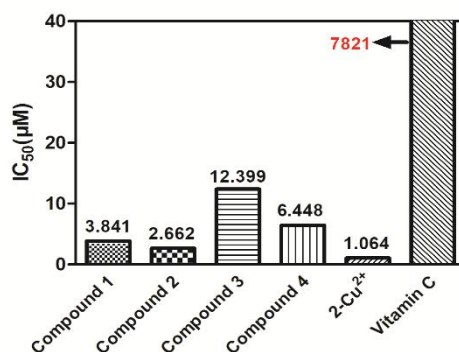


Figure 4. Antioxidant activity of compounds **1-4**, **2-Cu²⁺**, and vitamin C.

Chem. Biodiversity

The Docking Studies

Molecular docking is a useful tool for complex interactions between the receptor and ligand.^[36,37] To further investigate the binding ability and mode of compounds **1-4** to cholinesterase, molecular modeling was carried out by the Cdocker module of Discovery studio (DS, V7.6). As shown in Figure 5-8, the docking results indicated that **1-4** could bind with the CAS, mid-gorge site and PAS of AChE. In the bottom of the gorge, the terminal amine of **1-2** and **4** were observed to bind to the CAS via a carbon-hydrogen bond interaction between His 440 (2.73 Å, 2.66 Å and 2.83 Å). The pyrrolidine ring in **2** and piperidine ring in **4** were observed to bind to the CAS via the carbon-hydrogen bond and π -alkyl interaction between Trp84 and Phe330. However, the oxygen atom of morpholinyl in **3** might reduce the electron density of terminal amine via the electron-withdrawing effect, thus affecting the protonation of amine and the interaction between **2** and AChE. So, **3** exhibited much weaker affinity with AChE than the other compounds. Cdocker interaction energy was used to evaluate the binding affinity.^[38] The higher the -Cdocker interaction energy, the greater the binding affinity between the acceptor and the ligand is. The docking scores of the compounds with AChE (Table 2) showed that among compounds **1-4**, **2** had the strongest affinity, but was slightly weaker than donepezil (-Cdocker interaction energy = 50.8019 kcal·mol⁻¹). The sequence of -Cdocker interaction energy was **2** > **4** > **1** > **3**.

The results showed that the inhibitory potency against AChE was closely related with the tertiary amine groups. The tertiary amine groups could improve the affinity of xanthone to cholinesterase. The higher the pK_a value, the stronger the binding energy was. The order of the pK_a value of the tertiary amine group was pyrrolealkyl (pK_a = 11.27) > piperidinyl (pK_a = 11.22) > dimethylamino (pK_a = 10.64) > morpholinyl (pK_a = 8.36). So compound **2** showed the highest inhibition and binding energy to AChE, which was consistent with the results of in vitro experiments.

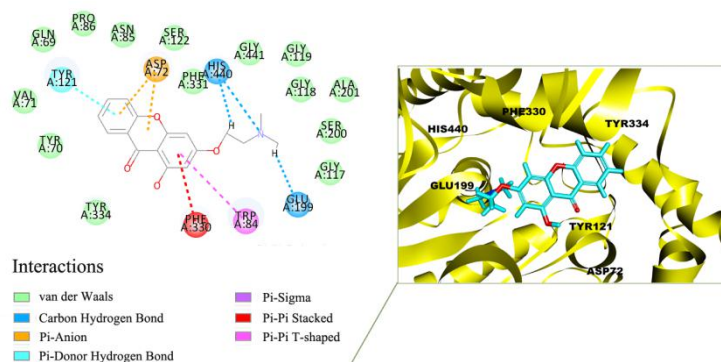


Figure 5. Molecular modeling of compound **1** with AChE.

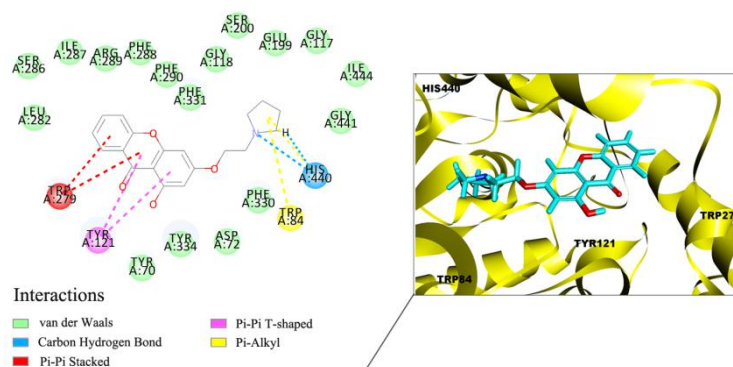


Figure 6. Molecular modeling of compound **2** with AChE.

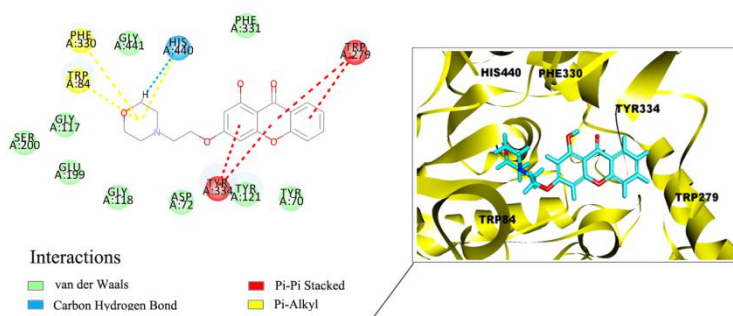


Figure 7. Molecular modeling of compound **3** with AChE.

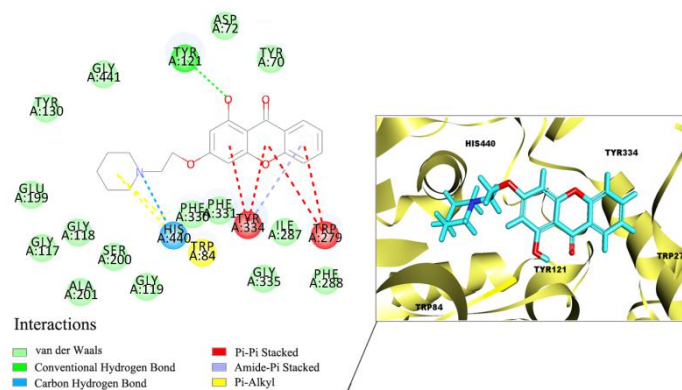


Figure 8. Molecular modeling of compound **4** with AChE.

As shown in Table 2, the affinities of **2** to AChE and BuChE were significantly different, suggesting that **2** could be used as a selective AChE inhibitor. And the affinities of **4** to AChE and BuChE were comparative, indicating that **4** could be used as a double inhibitor. Molecular modeling figures (Figure S6-S7) illustrate the difference between **2** and **4** with BuChE. Compound **4** had richer binding modes with BuChE than **2** such as electrostatic attraction (attractive charge). Furthermore, **4** bound to the active site of BuChE more strongly since it could interact with the aromatic ring of Trp82 by face to face π - π interactions. The docking result was useful to understand the results of in vitro experiments.

Table 2. -Cdocker interaction energy of compounds (kcal·mol⁻¹).

Compounds	-Cdocker interaction energy (AChE)	-Cdocker interaction energy (BuChE)
1	39.1120	37.9944
2	41.3323	32.7270
3	39.8513	38.2094
4	40.4663	41.5472
1,3-DHX	30.2141	27.7674

Prediction of absorption and BBB permeability

The drug-likeness and blood brain barrier permeability are important for studying on drugs of central nervous system (CNS). In recent years, rule of 5^[39] (including H-bond donors < 5, H-bond acceptors < 10, the molecular weight (MW) < 500, CLogP < 5 and rotatable bonds < 10) and polar surface area < 70 Å²^[40] have been used to predict the absorption and BBB permeability of compounds. The H-bond acceptors, H-bond donors and rotatable bonds values were calculated by the admet SAR server.^[41] The MW, ClogP and polar surface area were calculated by ChemDraw 12.0. The prediction of BBB penetration was also evaluated by the admet SAR server. As shown in Table 3, the evaluation data of compounds **1-4** satisfied the above rules and are similar to standard drugs (donepezil). It suggested that **1-4** had good absorption and permeability.

Table 3. The evaluated data of the compounds **1-4** and donepezil.

	1	2	3	4	donepezil
MW	299.8	325.8	341.1	339.1	379.5
ClogP	3.7	4.4	3.8	4.9	4.6
H-bond acceptors	5	5	6	5	4
H-bond donors	1	1	1	1	0
Rotatable bonds	4	4	4	4	6
Polar surface area (Å ²)	59	59	68	59	39
BBB penetration	+	+	+	+	+

Conclusions

In summary, four novel xanthone derivatives were synthesized. In vitro results showed that **1-4** displayed inhibitory activity for AChE. Moreover, these compounds showed strong antioxidant activity and metal chelating property. And the results from ChemDraw and the admet SAR server indicated that **1-4** had good absorption and permeability. **2** exhibited the highest AChE inhibition activity, selectivity for inhibition of AChE over BuChE and antioxidant activity. The enzyme kinetics and molecular modeling studies indicated that the xanthone scaffold of **2** can bind the PAS, while the introduced terminal amine group could interact with CAS. Especially, after coordinating to metal, **2** displayed much better bioactivities possibly due to the synergetic effect. So, compounds **1-4**, especially **2**, have potential to be developed into new anti-Alzheimer's agents.

Experimental*Materials and methods*

Chem. Biodiversity

All chemicals were purchased from Aladdin Reagent Co. Ltd. (Shanghai, China) without being purified before use. AChE, BuChE, bull serum albumin (BSA), 5,5'-dithiobis(2-nitrobenzoic acid) (DTNB), acetylthiocholine iodide (ATCI) and butylthiocholine iodide (BTCl) were purchased from Sigma-Aldrich LLC. (Shanghai, China). ¹H NMR spectra were recorded using TMS as the internal standard in CDCl₃ on a Bruker 400 MHz instrument (Bruker, Karlsruhe, Germany). Elemental analyses were performed at CNQO (CSIC, Spain). Mass spectrometry (MS) was acquired on a Quadrupole 6120 MS spectrometer (Agilent Technologies Co., Ltd., USA). Melting points were measured on the X-4 micro melting point meter (Shanghai precision scientific instrument Co. Ltd., China). UV spectra were recorded on a Shimadzu UV-2401 PC spectrophotometer. The absorbance in enzyme tests was measured at 405 nm using a microplate reader (TECAN, infinite m200 pro).

1,3-dihydroxy xanthone

100 mL previously prepared Eaton's reagent was added slowly into the mixture of dehydrated phloroglucinol (50 mmol, 6.31 g) and salicylic acid (50 mmol, 6.92 g). Then, the reaction mixture was kept stirring at 75°C until TLC indicated completion. After cooling to room temperature, the reaction mixture was poured into crushed ice and stirred for 3 h.^[26] The resulting solid was filtered, washed with distilled water. The dried solid was purified by silica gel column chromatography to obtain a pale yellow solid, yield 75 %.

General procedures for the preparation of compounds 1-4.

A mixture of 1,3-DHX (C₁₃H₈O₄, 2.0 mmol, 0.46g) and K₂CO₃ (6.0 mmol, 0.83 g) was dissolved in anhydrous acetone. The mixture was refluxed under stirring at 60°C. After 30 minutes, KI (3.0 mmol, 0.50 g) and amines chloride hydrochloride salt (6.0 mmol) were added to the reaction solution. The reaction mixture was kept stirring until TLC indicated completion.^[27] The crude products were purified by chromatography on a silicagel column and recrystallized to obtain compounds **1-4** as yellow solids.

3-(2-(dimethylamino)ethoxy)-1-hydroxy-9H-xanthen-9-one (1)

Yellow crystals, yield 42 %, m.p. 93-95 °C. ¹H NMR (CDCl₃) δ (ppm): 12.71 (s, 1H), 8.06 (dd, *J* = 7.87, 1.14 Hz, 1H), 7.84-7.79 (m, 1H), 7.51 (d, *J* = 8.38 Hz, 1H), 7.42 (t, *J* = 7.50 Hz, 1H), 6.51 (d, *J* = 2.06 Hz, 1H), 6.29 (d, *J* = 2.07 Hz, 1H), 4.12 (t, *J* = 5.69 Hz, 2H), 2.62 (t, *J* = 5.67 Hz, 2H), 2.21 (s, 6H); ¹³C NMR (DMSO) δ (ppm): 179.9, 165.7, 162.4, 157.0, 155.2, 135.6, 125.1, 124.3, 119.6, 117.5, 102.9, 97.3, 92.9, 66.7, 57.2, 45.4. MS: 299.8 ([M + H]⁺). Anal. calc. for C₁₇H₁₇NO₄ (299.12): C 68.22, H 5.72, N 4.68; found: C 68.02, H 5.49, N 4.72. IR (KBr) ν(cm⁻¹): 3426, 2923, 1660, 1602, 1467, 1292, 1229, 1164, 925, 749.

3-(2-(pyrrolidinyl)ethoxy)-1-hydroxy-9H-xanthen-9-one (2)

Yellow crystals, yield 20 %, m.p. 112-114 °C. ¹H NMR (CDCl₃) δ (ppm): 12.86 (s, 1H), 8.24 (dd, *J* = 1.0, 7.5 Hz, 1H), 7.74-7.68 (m, 1H), 7.43 (d, *J* = 8.42 Hz, 1H), 7.38 (t, *J* = 7.52 Hz, 1H), 6.46 (d, *J* = 2.08 Hz, 1H), 6.37 (d, *J* = 2.08 Hz, 1H), 4.20 (t, *J* = 5.86 Hz, 2H), 2.94 (t, *J* = 5.85 Hz, 2H), 2.64 (m, 4H), 1.89-1.76 (m, 4H); ¹³C NMR (CDCl₃) δ (ppm): 180.8, 166.0, 163.5, 157.7, 156.1, 135.0, 125.9, 124.0, 120.7, 117.6, 104.0, 97.6, 93.4, 67.7, 54.8, 54.7, 23.5. MS: 325.8 ([M + H]⁺). Anal. calc. for C₁₉H₁₉NO₄ (325.13): C

Chem. Biodiversity

70.14, H 5.89, N 4.31; found: C 70.01, H 5.82, N 4.52. IR (KBr) $\nu(\text{cm}^{-1})$: 3406, 2953, 1658, 1601, 1465, 1292, 1234, 1161, 936, 754.

3-(2-(morpholinyl)ethoxy)-1-hydroxy-9H-xanthen-9-one (3)

Yellow crystals, yield 16 %, m.p.131-136 °C. ^1H NMR (CDCl_3) δ (ppm): 12.86 (s, 1H), 8.25 (dd, $J = 7.92$, 1.33 Hz, 1H), 7.74-7.69 (m, 1H), 7.43 (d, $J = 8.43$ Hz, 1H), 7.38 (t, $J = 7.54$ Hz, 1H), 6.44 (d, $J = 2.17$ Hz, 1H), 6.35 (d, $J = 2.16$ Hz, 1H), 4.20 (t, $J = 5.66$ Hz, 2H), 3.76-3.73 (m, 4H), 2.84 (t, $J = 5.65$ Hz, 2H), 2.61-2.57 (m, 4H); ^{13}C NMR (CDCl_3). δ (ppm): 180.9, 163.6, 157.8, 156.1, 135.1, 125.9, 124.1, 120.7, 117.7, 104.1, 97.5, 93.4, 66.7, 66.4, 57.2, 54.0. MS: 341.8 ($[\text{M} + \text{H}]^+$). Anal. calc. for $\text{C}_{17}\text{H}_{17}\text{NO}_4$ (341.13): C 66.85, H 5.61, N 4.10; found: C 66.78, H 5.49, N 4.06. IR (KBr) $\nu(\text{cm}^{-1})$: 3470, 2969, 1646, 1608, 1421, 1297, 1231, 1164, 917, 764.

3-(2-(piperidinyl)ethoxy)-1-hydroxy-9H-xanthen-9-one (4)

Yellow crystals, yield 33 %, m.p.106-110 °C. ^1H NMR (CDCl_3) δ ppm: 12.83 (s, 1H), 8.30 (dd, $J = 0.8$, 7.6 Hz, 1H), 7.79-7.60 (m, 1H), 7.41 (d, $J = 8.41$ Hz, 1H), 7.36 (t, $J = 7.54$ Hz, 1H), 6.43 (d, $J = 2.01$ Hz, 1H), 6.34 (d, $J = 2.00$ Hz, 1H), 2.82 (t, $J = 5.92$ Hz, 2H), 4.19 (t, $J = 5.93$ Hz, 2H), 1.50-1.43 (m, 2H), 2.53 (s, 4H), 1.62 (td, $J = 11.03$, 5.58 Hz, 4H); ^{13}C NMR (CDCl_3) δ (ppm): 180.9, 166.1, 163.6, 157.8, 156.2, 135.1, 126.0, 124.1, 120.8, 117.7, 104.1, 97.7, 93.5, 66.8, 57.6, 55.2, 26.0, 24.2. MS: 339.9 ($[\text{M} + \text{H}]^+$). Anal. calc. for $\text{C}_{20}\text{H}_{21}\text{NO}_4$ (339.15): C 70.78, H 6.24, N 4.13; found: C 70.58, H 6.12, N 4.10. IR (KBr) $\nu(\text{cm}^{-1})$: 3470, 2932, 1650, 1606, 1416, 1289, 1233, 1169, 912, 755.

Metal chelation

The chelating studies were performed with a UV-Vis spectrophotometer with wavelength ranging from 200 to 400 nm. The chelating abilities of compounds **1-4** and mole ratio of Cu^{2+} and Fe^{3+} complexes were measured by a molar ratio method through titrating the methanol solution of compounds with ascending amounts of $\text{CuCl}_2 \cdot 2\text{H}_2\text{O}$ and $\text{FeCl}_3 \cdot 6\text{H}_2\text{O}$.^[42] The absorption spectra were recorded at room temperature. The reaction was stopped after the mole fraction of the metal ion to compounds **1-4** reached 1.

Inhibition of ChEs

The inhibitory activities were evaluated by Ellman's method.^[29] All test compounds were dissolved in DMSO and diluted to different concentrations with buffer solution A (Tris-HCl, 50 mM, pH = 8.0). The final concentration of DMSO was less than 0.5 %. Buffer solution B (0.02% BSA in buffer A, 30 μL), DTNB (2.4 mM, 10 μL), AChE or BuChE (10 μL) and different concentrations of the test compounds (10 μL) were incubated at 37 °C for 10 min. Then ATCI (1.6 mM, 10 μL) or BTCl (1.6 mM, 10 μL) was added as the substrate. After incubation for another 15 min at 37 °C, SDS (0.4 %, 30 μL) was added to stop the reaction. The IC_{50} values were calculated using SPSS.

Kinetic of AChE inhibition

Kinetic characterization of AChE was performed using Ellman's method. Buffer solution B (30 μL), DTNB (2.4 mM, 10 μL), AChE (10 μL) and 10 μL different concentrations (1.2 μM , 2.4 μM , 5.0 μM) of

Chem. Biodiversity

compound **2** were pre-incubated at 37 °C for 10 min. Then, different concentrations of ACTI (20 µL, 0.32 mM, 0.48 mM, 0.64 mM, 0.8 mM, 0.96 mM) were added. After incubation for another 15 min at 37 °C, SDS (30 µL, 0.4 %) was added to stop the reaction. The absorbance was measured at 405 nm using a microplate reader.^[43] The data were analyzed using Origin 2018.

Antioxidant ability

The ability of the compounds to scavenge hydroxyl radical was tested by the Fenton reaction.^[32] The reaction mixture was composed of safranin T solution (0.5 mM, 20 µL), EDTA-Fe²⁺ (10 mM, 10 µL), different concentrations of **2** (20 µL), buffer solution (Tris-HCl, pH=7.4, 30 µL,) and H₂O₂ solution (3%, 40 µL). The absorbance at 520 nm was measured using a microplate reader and analyzed by Origin 2018.

Molecular modeling study

Molecular docking studies were performed using Discovery studio (DS, V7.6). The X-ray crystallographic structures of AChE with donepezil (PDB code 1EVE) and BuChE (PDB code 1POI) were obtained from the PDB. The 3D structures of **1-4** were constructed by ChemDraw 12.0. Hydrogenation, completion the loop chain, and adding CHARMM force field to the protein were completed with the protein preparation tool. Ligands were optimized with minimizing ligand program. The active site was selected as an amino acid in the range of 5 Å around the original ligand (donepezil), and the radius of the SBD_Site_Sphere is 15.0.^[44] To validate the docking reliability, co-crystallized ligand donepezil was first re-docked to the binding site of AChE.^[45] The Cdocker module was used for docking compounds **1-4** into the active site of the corresponding protein. The interactions with binding pocket residues were analyzed and evaluated by Cdocker interaction energy.

Supplementary Material

Supporting information for this article is available on the WWW under <http://dx.doi.org/10.1002/MS-number>.

Acknowledgements

This work was supported by National Natural Science Foundation of China (NSFC, No.81503462).

Author Contribution Statement

Aihong Yang contributed to the designing of the experiments, interpreting of the results as well as preparing the manuscript. Qiao Yu, carried out data analyses, molecular docking, and conducted the biological assays. Hui Ju and Lulu Song contributed to the synthesis and characterization of all compounds. Xiaodi Kou and Rui Shen supervised all biological assays, discussed the results and wrote the manuscript. All the authors revised the final manuscript together.

References

- [1] C. Nance, A. Ritter, J. B. Miller, B. Lapin, S. J. Banks, 'The pathology of rapid cognitive decline in clinically diagnosed Alzheimer's disease', *J. Alzheimer's Dis.* **2019**, *70*, 983-993.

Chem. Biodiversity

- [2] G. Si, S. Zhou, G. Xu, J. Wang, B. Wu, S. Zhou, 'A curcumin-based NIR fluorescence probe for detection of amyloid-beta (A β) plaques in Alzheimer's disease', *Dyes Pigm.* **2019**, *163*, 509-515.
- [3] L. C. Dos Santos Picanco, P. F. Ozela, M. de Fatima de Brito Brito, A. A. Pinheiro, E. C. Padilha, F. S. Braga, C. H. T. de Paula da Silva, C. B. R. Dos Santos, J. M. C. Rosa, L. I. da Silva Hagemelin, 'Alzheimer's disease: A review from the pathophysiology to diagnosis, new perspectives for pharmacological treatment'. *Curr. Med. Chem.* **2018**, *25*, 3141-3159.
- [4] R. T. Bartus, R. L. Dean 3rd, B. Beer, A. S. Lippa, 'The cholinergic hypothesis of geriatric memory dysfunction', *Science* **1982**, *217*, 408-417.
- [5] C. Cheignon, M. Tomas, D. Bonnefont-Rousselot, P. Faller, C. Hureau, F. Collin, 'Oxidative stress and the amyloid beta peptide in Alzheimer's disease', *Redox Bio.* **2018**, *14*, 450-464.
- [6] P. A. Adlard, A. I. Bush, 'Metals and Alzheimer's Disease: How Far Have We Come in the Clinic?', *J. Alzheimer's Dis.* **2018**, *62*, 1369-1379.
- [7] A. Castro, A. Martinez, 'Targeting beta-amyloid pathogenesis through acetylcholinesterase inhibitors', *Curr. Pharm. Des.* **2006**, *12*, 4377-4387.
- [8] Z. Gazova, O. Soukup, V. Sepsova, K. Siposova, L. Drtinova, P. Jost, K. Spilovska, J. Korabecny, E. Nepovimova, D. Fedunova, M. Horak, M. Kaniakova, Z. J. Wang, A. K. Hamouda, K. Kuca, 'Multi-target-directed therapeutic potential of 7-methoxytacrine-adamantylamine heterodimers in the Alzheimer's disease treatment', *Biochim. Biophys. Acta, Mol. Basis Dis.* **2017**, *1863*, 607-619.
- [9] S. S. Xie, J. S. Lan, X. Wang, Z. M. Wang, N. Jiang, F. Li, J. J. Wu, J. Wang, L. Y. Kong, 'Design, synthesis and biological evaluation of novel donepezil-coumarin hybrids as multi-target agents for the treatment of Alzheimer's disease', *Bioorg. Med. Chem.* **2016**, *24*, 1528-1539.
- [10] N. N. Nalivaeva, A. J. Turner, 'AChE and the amyloid precursor protein (APP)-cross-talk in Alzheimer's disease', *Chem.-Biol. Interact.* **2016**, *259*, 301-306.
- [11] D. J. Hayne, S. Lim, P. S. Donnelly, 'Metal complexes designed to bind to amyloid-beta for the diagnosis and treatment of Alzheimer's disease', *Chem. Soc. Rev.* **2014**, *43*, 6701-6715.
- [12] M. P. Cuajungco, K. Y. Fagét, X. Huang, R. E. Tanzi, A. I. Bush, 'Metal chelation as a potential therapy for Alzheimer's disease', *Ann. N. Y. Acad. Sci.* **2010**, *920*, 292-304.
- [13] F. Gu, M. Zhu, J. Shi, Y. Hu, Z. Zhao, 'Enhanced oxidative stress is an early event during development of Alzheimer-like pathologies in presenilin conditional knock-out mice', *Neurosci. Lett.* **2008**, *440*, 44-48.
- [14] M. Rosini, E. Simoni, M. Bartolini, A. Tarozzi, R. Matera, A. Milelli, P. Hrelia, V. Andrisano, M. L. Bolognesi, C. Melchiorre, 'Exploiting the lipoic acid structure in the search for novel multitarget ligands against Alzheimer's disease', *Eur. J. Med. Chem.* **2011**, *46*, 5435-5442.
- [15] S. Pervaiz, S. Mutahir, I. Ullah, M. Ashraf, X. Liu, S. Tariq, B. J. Zhou, M. A. Khan, 'Organocatalyzed solvent free and efficient synthesis of 2,4,5-trisubstituted imidazoles as potential acetylcholinesterase inhibitors for Alzheimer's disease', *Chem. Biodiversity* **2020**, *17*, 1-21.

Chem. Biodiversity

- [16] S. Mutahir, J. Jończyk, M. Bajda, I. U. Khan, M. A. Khan, N. Ullah, M. Ashraf, Qurat-ul-Ain, S. Riaz, S. Hussain, M. Yar. 'Novel biphenyl bis-sulfonamides as acetyl and butyrylcholinesterase inhibitors: Synthesis, biological evaluation and molecular modeling studies', *Bioorg. Chem.* **2016**, 64, 13-20.
- [17] J. Ruan, C. Zheng, Y. Liu, L. Qu, H. Yu, L. Han, Y. Zhang, T. Wang, 'Chemical and biological research on herbal medicines rich in xanthenes', *Molecules* **2017**, 22, 1-19.
- [18] T. Tizziani, M. Pereira, D. Venzke, F. C. Missau, A. P. Ruani, D. F. Montagner, M. G. Pizzolatti, G. A. Micke, I. M. C. Brighente, 'A new xanthone as a chemical marker of four Polygala species (Polygalaceae)', *Biochem. Syst. Ecol.* **2018**, 78, 46-48.
- [19] M. I. Chung, J. R. Weng, J. P. Wang, C. M. Teng, C. N. Lin, 'Antiplatelet and anti-inflammatory constituents and new oxygenated xanthenes from *Hypericum geminiflorum*', *Planta Med.* **2002**, 68, 25-29.
- [20] G. C. Ee, S. Daud, S. A. Izzaddin, M. Rahman, 'Garcinia mangostana: a source of potential anti-cancer lead compounds against CEM-SS cell line', *J. Asian Nat. Prod. Res.* **2008**, 10, 475-479.
- [21] C. M. Santos, M. Freitas, D. Ribeiro, A. Gomes, A. M. Silva, J. A. Cavaleiro, E. Fernandes, '2,3-diaryl-xanthenes as strong scavengers of reactive oxygen and nitrogen species: a structure-activity relationship study', *Bioorg. Med. Chem.* **2010**, 18, 6776-6784.
- [22] K. Y. Khaw, S. B. Choi, S. C. Tan, H. A. Wahab, K. L. Chan, V. Murugaiyah, 'Prenylated xanthenes from mangosteen as promising cholinesterase inhibitors and their molecular docking studies', *Phytomedicine* **2014**, 21, 1303-1309.
- [23] T. Wezeman, S. Brase, K. S. Masters, 'Xanthone dimers: a compound family which is both common and privileged', *Nat. Prod. Rep.* **2015**, 32, 6-28.
- [24] C. A. Menéndez, B. Biscussi, S. Accordino, A. P. Murray, D. C. Gerbino, G. A. Appignanesi, 'Design, synthesis and biological evaluation of 1,3-dihydroxyxanthone derivatives: Effective agents against acetylcholinesterase', *Bioorg. Chem.* **2017**, 75, 201-209.
- [25] J. Qin, W. Lan, Z. Liu, J. Huang, H. Tang, H. Wang, 'Synthesis and biological evaluation of 1, 3-dihydroxyxanthone mannich base derivatives as anticholinesterase agents', *Chem. Cent. J.* **2013**, 7, 1-11.
- [26] A. M. Das, M. Shaikh, S. Jana, 'Design, synthesis, and in vitro antibacterial screening of some novel 3-pentyloxy-1-hydroxyxanthone derivatives', *Med. Chem. Res.* **2013**, 23, 436-444.
- [27] Z. M. Yang, J. Huang, J. K. Qin, Z. K. Dai, W. L. Lan, G. F. Su, H. Tang, F. Yang, 'Design, synthesis and biological evaluation of novel 1-hydroxyl-3-aminoalkoxy xanthone derivatives as potent anticancer agents', *Eur. J. Med. Chem.* **2014**, 85, 487-497.
- [28] X. Kou, L. Song, Y. Wang, Q. Yu, H. Ju, A. Yang, R. Shen, 'Design, synthesis and anti-Alzheimer's disease activity study of xanthone derivatives based on multi-target strategy', *Bioorg. Med. Chem. Lett.* **2020**, 30, 126927.
- [29] G. L. Ellman, K. D. Courtney, V. Andres Jr, R. M. Featherstone, 'A new and rapid colorimetric determination of acetylcholinesterase activity', *Biochem. Pharmacol.* **1961**, 7, 88-95.

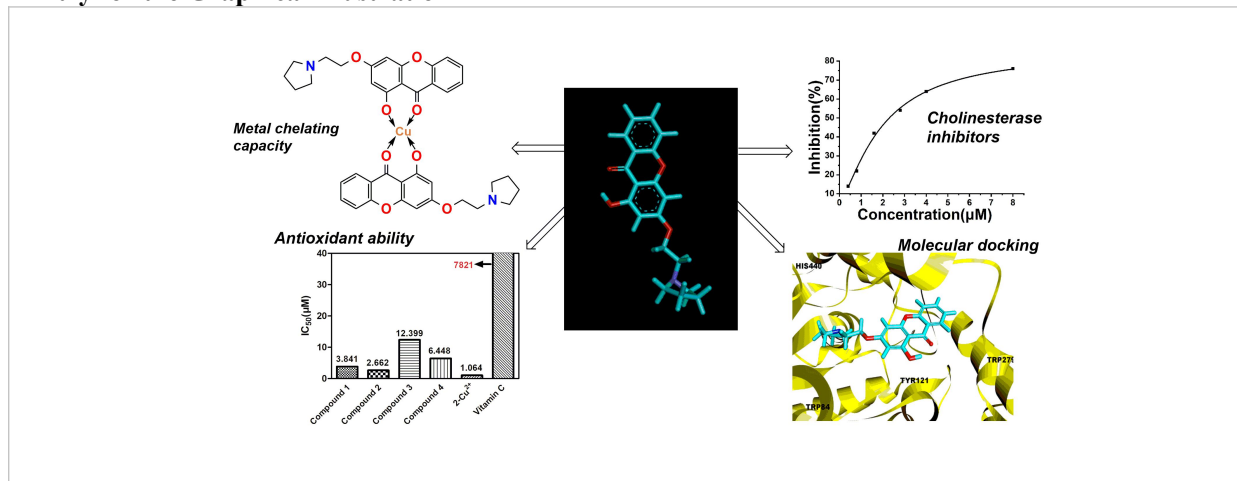
Chem. Biodiversity

- [30] G. L. Atkins, I. A. Nimmo, 'The reliability of Michaelis constants and maximum velocities estimated by using the integrated Michaelis-Menten equation', *Biochem. J.* **1973**, *135*, 779-784.
- [31] A. Bosak, D. M. Opsenica, G. Šinko, M. Zlatar, Z. Kovarik, 'Structural aspects of 4-aminoquinolines as reversible inhibitors of human acetylcholinesterase and butyrylcholinesterase'. *Chem.-Biol. Interact.* **2019**, *308*, 101-109.
- [32] L. P. Kuznetsova, E. B. Nikol'Skaya, E. E. Sochilina, M. D. Faddeeva, 'Inhibition of Human Blood Acetylcholinesterase and Butyrylcholinesterase by Some Alkaloids', *J. Evol. Biochem. Physiol.* **2002**, *38*, 35-39.
- [33] G. R. Zhao, H. M. Zhang, T. X. Ye, Z. J. Xiang, Y. J. Yuan, Z. X. Guo, L. B. Zhao, 'Characterization of the radical scavenging and antioxidant activities of danshensu and salvianolic acid B', *Food Chem. Toxicol.* **2008**, *46*, 73-81.
- [34] F. Yu, D. Xu, R. Lei, N. Li, K. Li, 'Free-radical scavenging capacity using the fenton reaction with rhodamine B as the spectrophotometric indicator', *J. Agric. Food Chem.* **2008**, *56*, 730-735.
- [35] L. G. Wade Jr, 'Organic chemistry', 8th ed, NY: Pearson Education Inc, New York, **2011**.
- [36] S. Mutahir, M. Yar, M. A. Khan, N. Ullah, S. A. Shahzad, I. U. Khan, R. A. Mehmood, M. Ashraf, R. Nasar, E. Pontiki, 'Synthesis, characterization, lipoyxygenase inhibitory activity and in silico molecular docking of biaryl bis(benzenesulfonamide) and indol-3-yl-hydrazide derivatives', *J. Iran Chem. Soc.* **2015**, *12*, 1123-1130.
- [37] S. Mutahir, M. A. Khan, I. U. Khan, M. Yar, M. Ashraf, S. Tariq, R. L. Ye, B. J. Zhou, 'Organocatalyzed and mechanochemical solvent-free synthesis of novel and functionalized bis-biphenyl substituted thiazolidinones as potent tyrosinase inhibitors: SAR and molecular modeling studies', *Eur. J. Med. Chem.* **2017**, *134*, 406-414.
- [38] B. H. Tan, N. Ahemad, Y. Pan, U. D. Palanisamy, L. Othmand, B. C. Yiape, C. E. Onge, 'Cytochrome P450 2C9-natural antiarthritic interactions: evaluation of inhibition magnitude and prediction from in vitro data', *Biopharm. Drug Dispos.* **2018**, *39*, 205-217.
- [39] C. A. Lipinski, F. Lombardo, B. W. Dominy, P. J. Feeney, 'Experimental and computational approaches to estimate solubility and permeability in drug discovery and development settings', *Adv. Drug Delivery Rev.* **2001**, *46*, 3-26.
- [40] J. Kelder, P. D. J. Grootenhuys, D. M. Bayada, L. P. C. Delbressine, J. P. Ploemen, 'Molecular surface as a dominating determinant for oral absorption and brain penetration of drugs', *Pharm. Res.* **1999**, *16*, 1514-1519.
- [41] M. Asadi, M. Ebrahimi, M. Mohammadi-Khanaposhtani, H. Azizian, S. Sepehri, H. Nadri, M. Biglar, M. Amanlou, B. Larijani, R. Mirzazadeh, N. Edraki, M. Mahdavi, 'Design, synthesis, molecular docking, and cholinesterase inhibitory potential of phthalimide-dithiocarbamate hybrids as new agents for treatment of Alzheimer's disease', *Chem. Biodiversity* **2019**, *16*, 1-13.
- [42] J. Hu, T. Pan, B. An, X. Li, X. Li, L. Huang, 'Synthesis and evaluation of clioquinol-rolipram/roflumilast hybrids as multitarget-directed ligands for the treatment of Alzheimer's disease', *Eur. J. Med. Chem.* **2019**, *163*, 512-526.

Chem. Biodiversity

- [43] Y. Guo, H. Yang, Z. Huang, S. Tian, Q. Li, C. Du, T. Chen, Y. Liu, H. Sun, Z. Liu, 'Design, synthesis, and evaluation of acetylcholinesterase and butyrylcholinesterase dual-target inhibitors against Alzheimer's diseases', *Molecules* **2020**, *25*, 1-21.
- [44] Z. Yu, S. Wu, W. Zhao, L. Ding, Y. Fan, D. Shiuan, J. Liu, F. Chen, 'Anti-Alzheimers activity and molecular mechanism of albumin-derived peptides against AChE and BChE', *Food Funct.* **2018**, *9*, 1173-1178.
- [45] S. Bhuvanendran, N. A. Hanapi, N. Ahemad, L. Othman, S. R. Yusof, M. F. Shaikh, 'Embelin, a potent molecule for Alzheimer's disease: a proof of concept from blood-brain barrier permeability, acetylcholinesterase inhibition and molecular docking studies', *Front. Neurosci.* **2019**, *13*, 1-10.

Entry for the Graphical Illustration



Twitter Text

Four xanthone derivatives were designed and synthesized. They are promising multi-targeted ligands against AD.